Supplementary Information

Ecological and environmental factors influencing exclusion patterns of phytoplankton size classes in lake systems

Sze-Wing To[1,2], Esteban Acevedo-Trejos[3], Sherwood Lan Smith[4,5], Subhendu Chakraborty[2], Agostino Merico[2,1]

[1] School of Science, Constructor University, Bremen, Germany

[2] Systems Ecology Group, Leibniz Centre for Tropical Marine Research (ZMT), Bremen, Germany

[3] Earth Surface Process Modelling, German Research Centre for Geoscience (GFZ), Potsdam, Germany

[4] Advanced Institute for Marine Ecosystem Change (WPI- AIMEC), JAMSTEC, Yokohama, Japan

[5] Earth SURFACE Research Centre, Research Institute for Global Change (JAMSTEC), Yokohama, Japan

***** *Corresponding author: sto@constructor.university*

1 Environmental forcing to the model

We adopted a theoretical mixing pattern based on a sinusoidal function for producing mixed layer depths with specific frequency and amplitude over an annual cycle (Fig. S1B). This allowed us to mimic contrasting mixing frequencies in lakes: constant, medium (Eq. S1) and high frequencies (Eq. S2). The sinusoidal functions applied to the model are as follow:

Constant [no mixing during the year] -

Medium frequency [4 mixings per year]
$$\left[\frac{(Z_m - Z_t)}{2} + Z_t\right] + \frac{(Z_m - Z_t)}{2} cos\left(\frac{DOY}{14.525}\right) \quad \text{(S1)}$$

High frequency [12 mixings per year]
$$\left[\frac{(Z_m - Z_t)}{2} + Z_t\right] + \frac{(Z_m - Z_t)}{2} cos\left(\frac{DOY}{4.825}\right) \quad \text{(S2)}$$

where

Z_m = mixing depth (m), 80m in the study

Z_t = thermocline depth (m), 2.5m in the study

DOY = day of year

In the model, in addition to remineralization of detritus, these different mixing frequencies strongly shape the patterns of nutrient variabilities supplied for biological processes (e.g. uptake by phytoplankton), in terms of $\varphi D + \lambda(N_0 - N)$, see Eq. 18. Hence, the phytoplankton in our model were subjected to fluctuating light (Fig. S1A) and nutrient resources (Fig. S8).

2 Calculation of phytoplankton community mean cell size

We tracked the emergent temporal changes in aggregate community size structure of the phytoplankton (Supp. Fig. S6) via the biomass-weighted community mean cell size, which is given by:

$$S_w = \frac{\sum_i^n P_i S_i}{\sum_i^n P_i}, \quad \text{(S3)}$$

where n is the total number of size classes. The value of S_w hence represents the dominance of a range of size classes instead of the presence of one single size class.

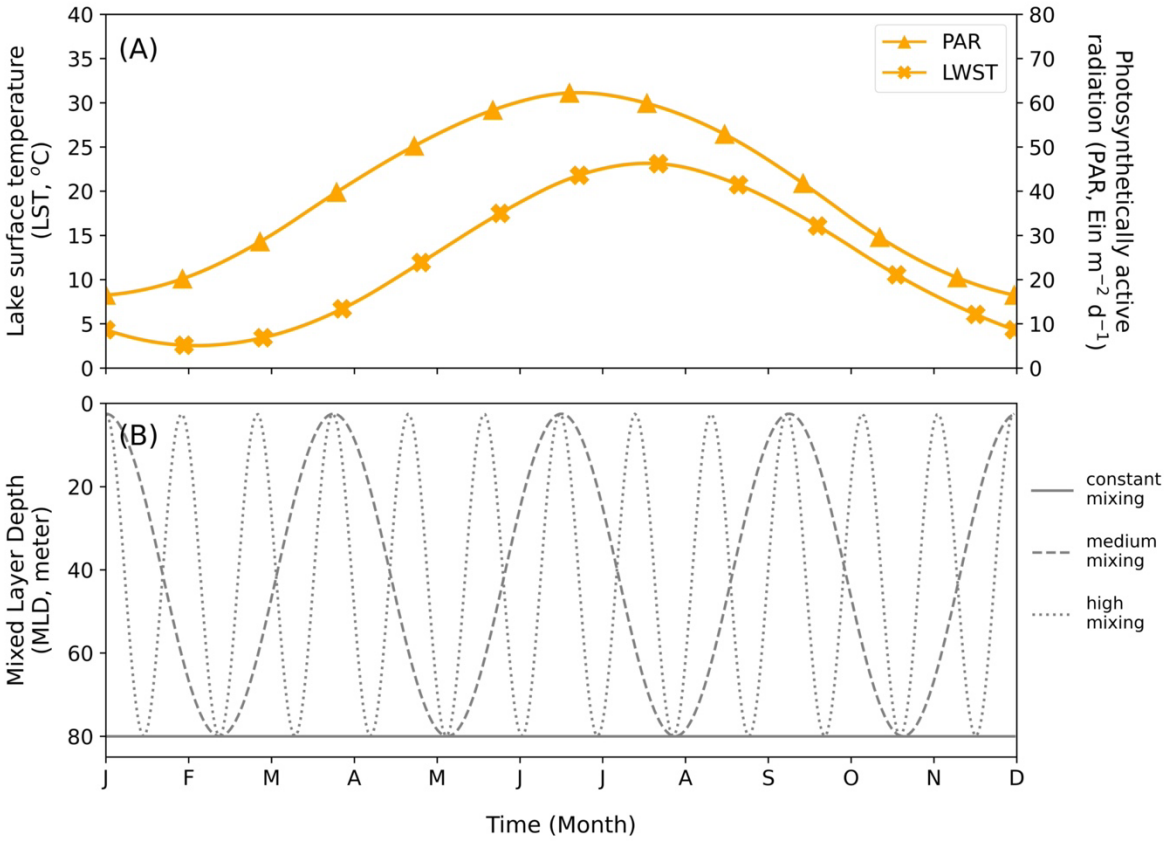

Figure S1. Annual variations of forcing variables used in the model. (A) The orange curves represent the interpolated functions of annual variation of lake surface temperature (LST) and Photosynthetically Active Radiance (converted from net shortwave solar irradiance, W m^{-2}). The triangle and cross symbols indicate, respectively, the projection data of LST and PAR from Layden et al. (2015). (B) Annual variations of the Mixed Layer Depth, which ranges between 2.5 and 80 meters, show three mixing scenarios: constant, medium, and high mixing frequencies.

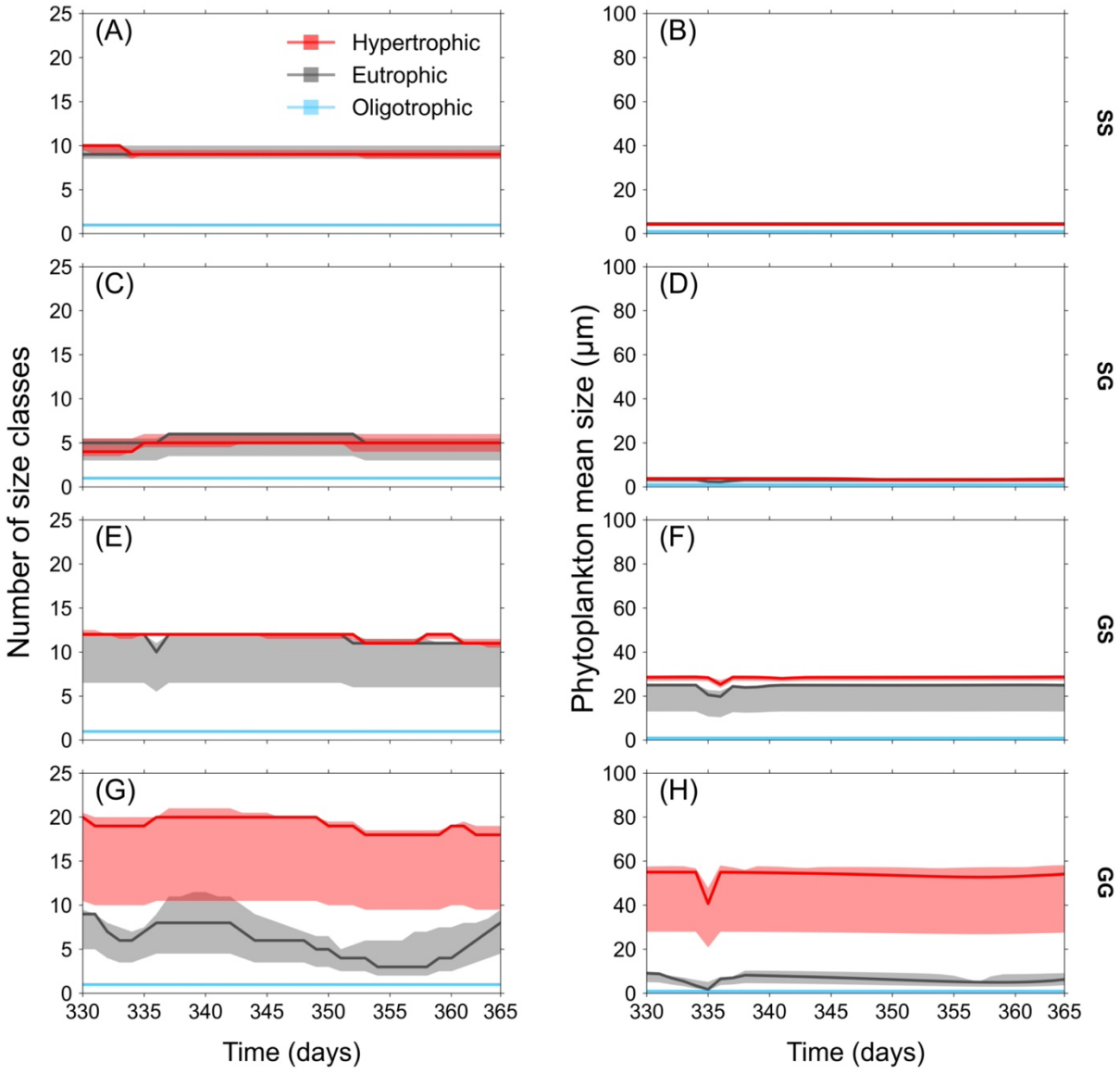

Figure S2. Number of phytoplankton size classes (A, C, E, and G) and phytoplankton mean size (B, D, F, and H) over day 330 to day 365 obtained under varying environmental conditions (nutrient regimes and mixing frequencies) and for different grazing scenarios. The colours indicate different nutrient regimes: light-blue for oligotrophic (1 µmol N L^{-1}); grey for eutrophic (15 µmol N L^{-1}); and red for hypertrophic (50 µmol N L^{-1}). For every nutrient regime, the continuous lines and the shaded areas represent, respectively, the median (50^{th} percentile) and the interquartile range (i.e. the 25^{th} and 75^{th} percentiles) of the results obtained with the three mixing frequencies (constant, medium, and high).

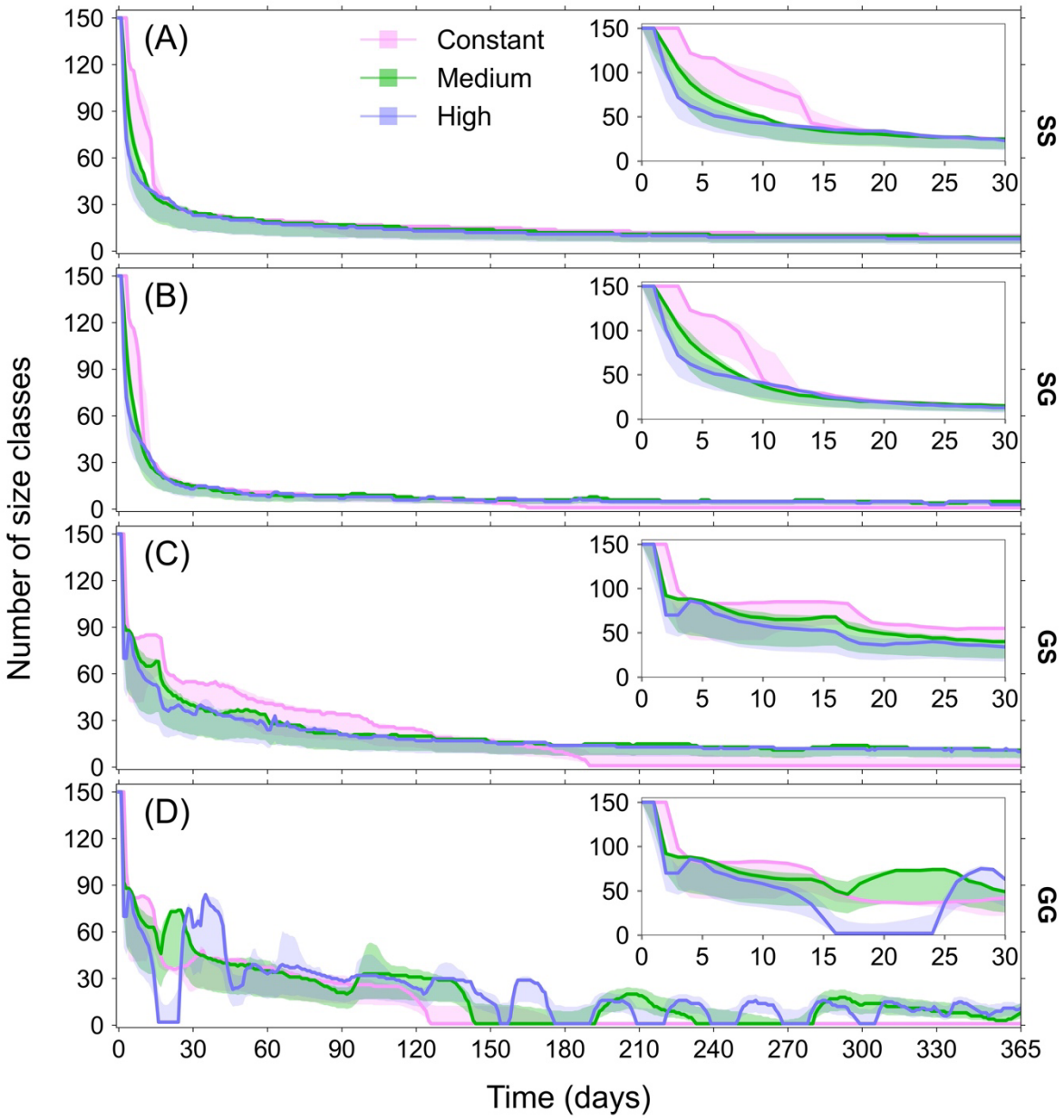

Figure S3. Exclusion patterns showing number of phytoplankton size classes under different mixing frequencies (constant: no mixing; medium: 4 mixing events per year; high: 12 mixing events per year) for different grazing scenarios: (A) 'SS'; (B) 'SG'; (C) 'GS'; and (D) 'GG'. The shaded areas and the lines mark, respectively, the interquartile range and the median of the three nutrient conditions (i.e. oligotrophic: 1 µmol N L^{-1}; eutrophic: 15 µmol N L^{-1}; and hypertrophic: 50 µmol N L^{-1}). The insets magnify the first 30 days.

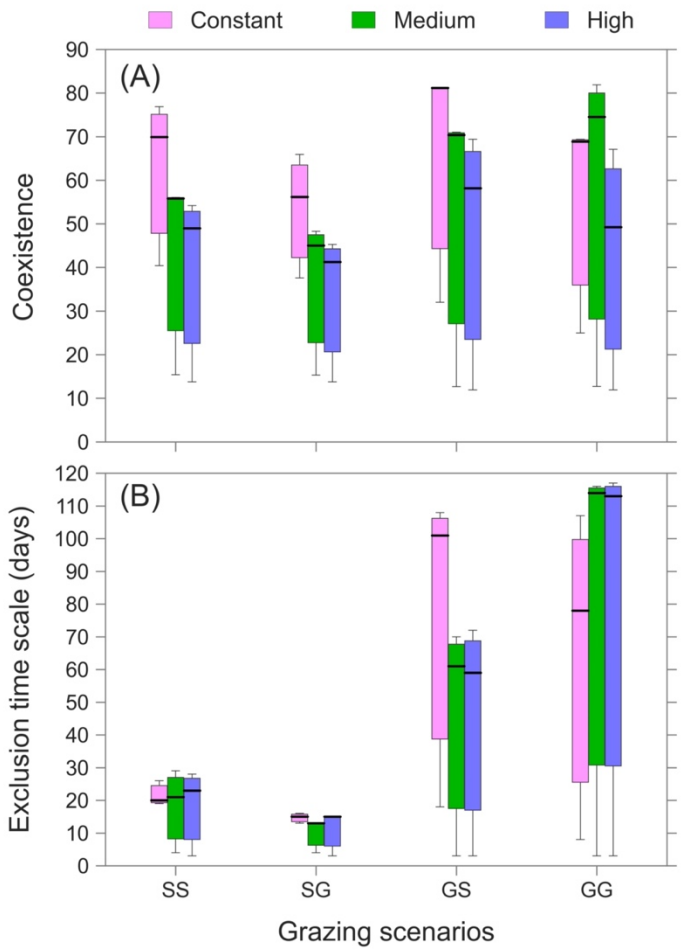

Figure S4. (A) Coexistence and (B) exclusion time scale at different mixing frequencies (colorization) for different grazing scenarios: SS, SG, GS, and GG. The width of each box-whisker represents the interquartile range and the dark line in the box indicates the median from three nutrient levels (oligotrophic, 1 μmol N L^{-1}; eutrophic, 15 μmol N L^{-1}; and hypertrophic, 50 μmol N L^{-1}).

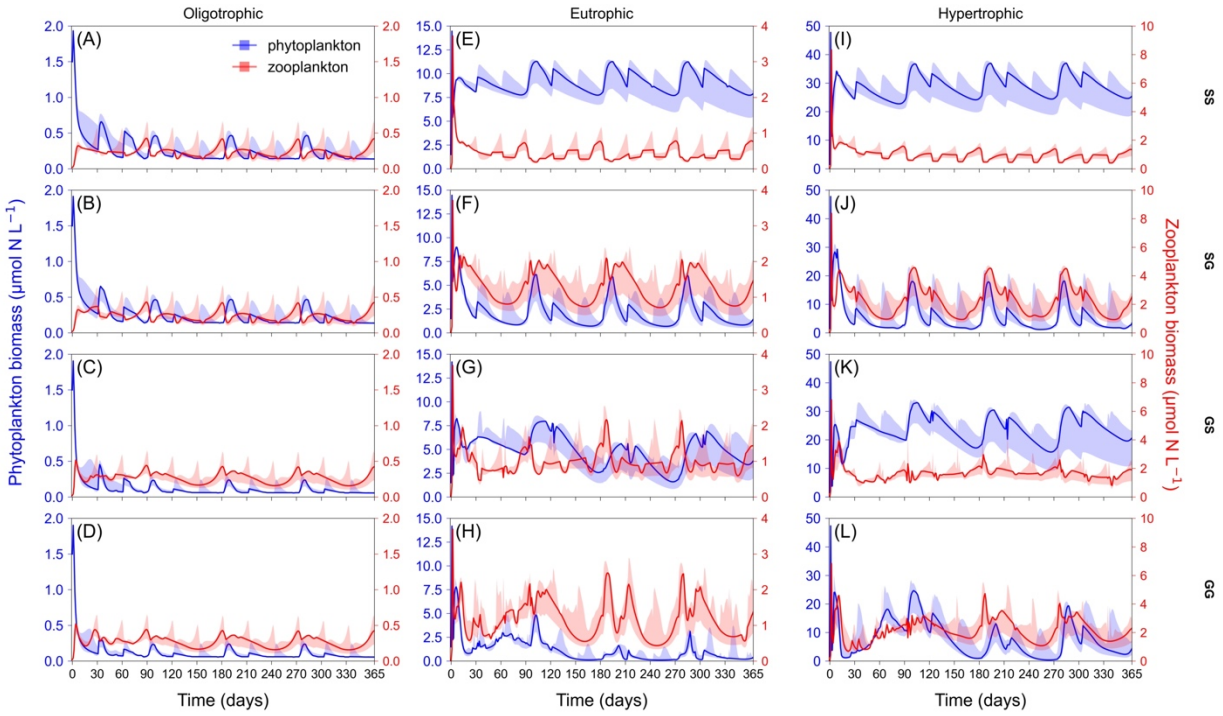

75

76 **Figure S5.** Phytoplankton and zooplankton biomass over time, shown in blue and red, respectively, reflecting
77 different predator-prey dynamics under varying mixing frequencies (shaded areas) for different nutrient regimes
78 (by column) and grazing scenarios (by row). The continuous lines and the shaded areas represent, respectively,
79 the median (50th percentile) and the interquartile range (i.e. the 25th and 75th percentiles) of the results obtained
80 with the three mixing frequencies (constant, medium, and high).

81

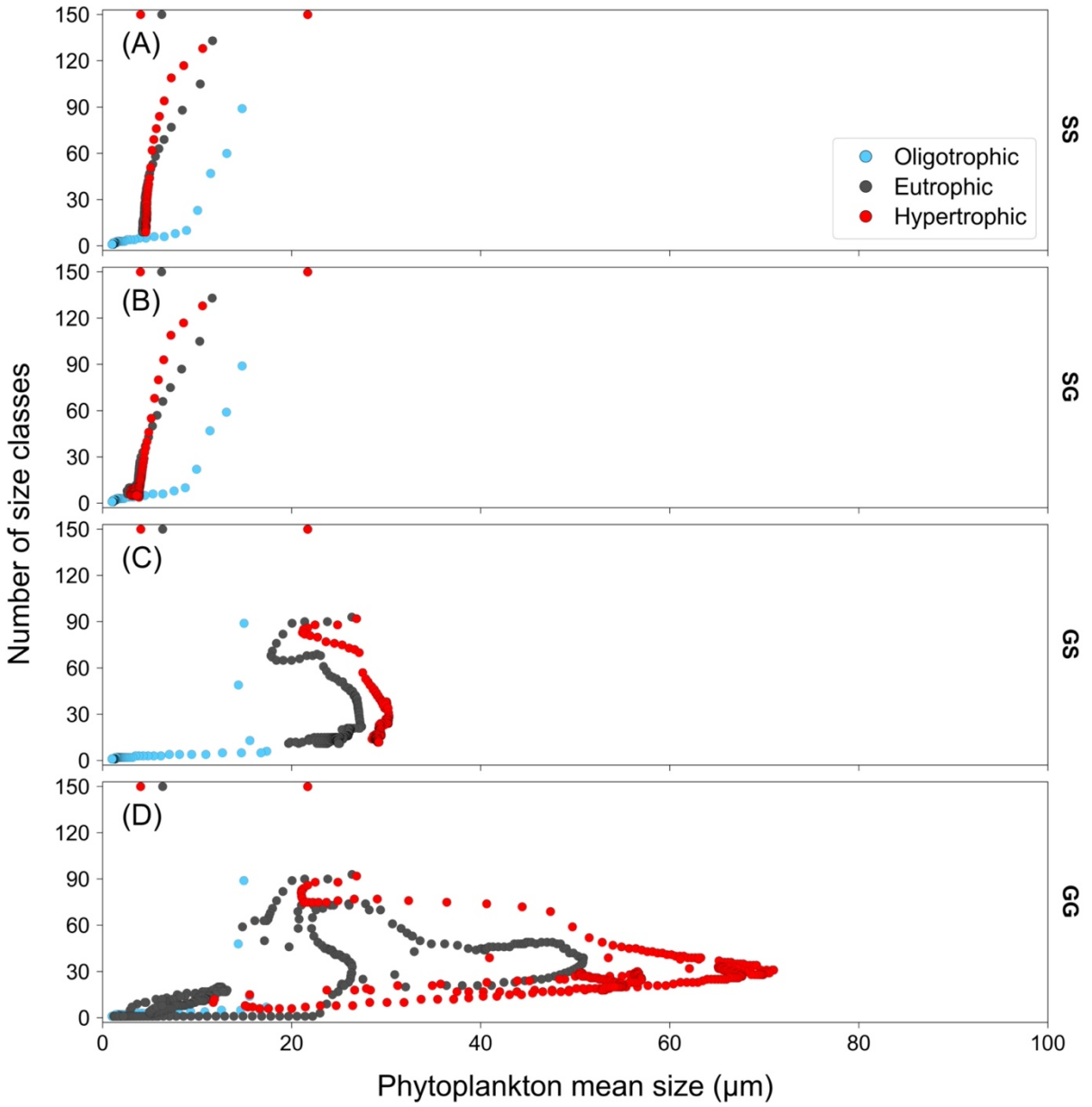

82

83 **Figure S6.** The number of size classes against phytoplankton mean cell size (see calculation in Supplementary
84 information 2) over 365 days, i.e. n=365. The results are under default allometric relationships and eutrophic
85 condition for different grazing scenarios: (A) SS, (B) SG, (C) GS, and (D) GG. The colours indicate different
86 nutrient regimes: light-blue for oligotrophic (1 μmol N L^{-1}); grey for eutrophic (15 μmol N L^{-1}); and red for
87 hypertrophic (50 μmol N L^{-1}). For these runs, the mixing frequency was fixed to medium.

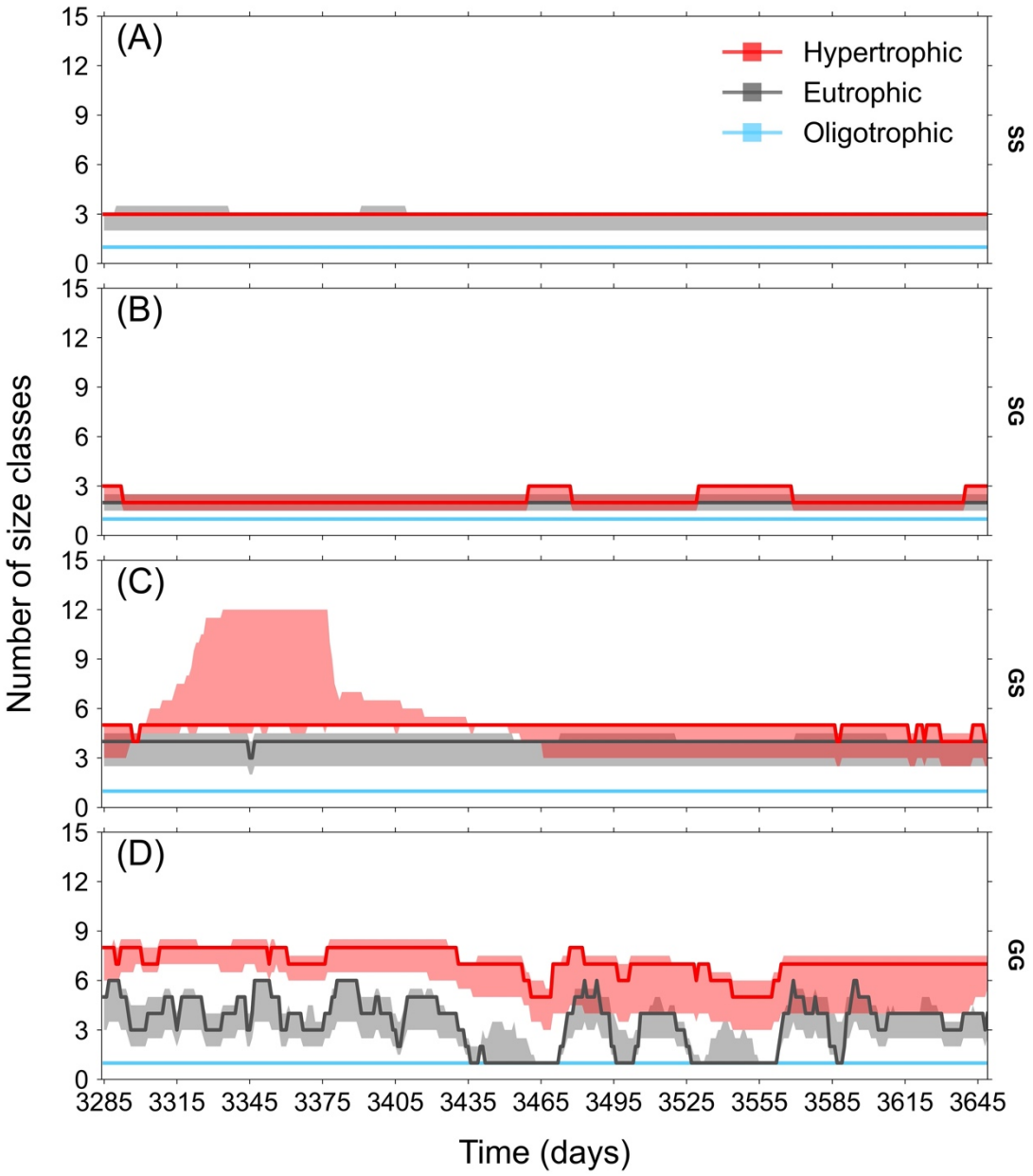

Figure S7. Number of phytoplankton size classes over steady-state (at the 10th year) for different grazing scenarios. The colours indicate different nutrient regimes: light-blue for oligotrophic (1 µmol N L^{-1}); grey for eutrophic (15 µmol N L^{-1}); and red for hypertrophic (50 µmol N L^{-1}). For every nutrient regime, the continuous lines and the shaded areas represent, respectively, the median (50th percentile) and the interquartile range (i.e. the 25th and 75th percentiles) of the results obtained with the three mixing frequencies (constant, medium, and high).

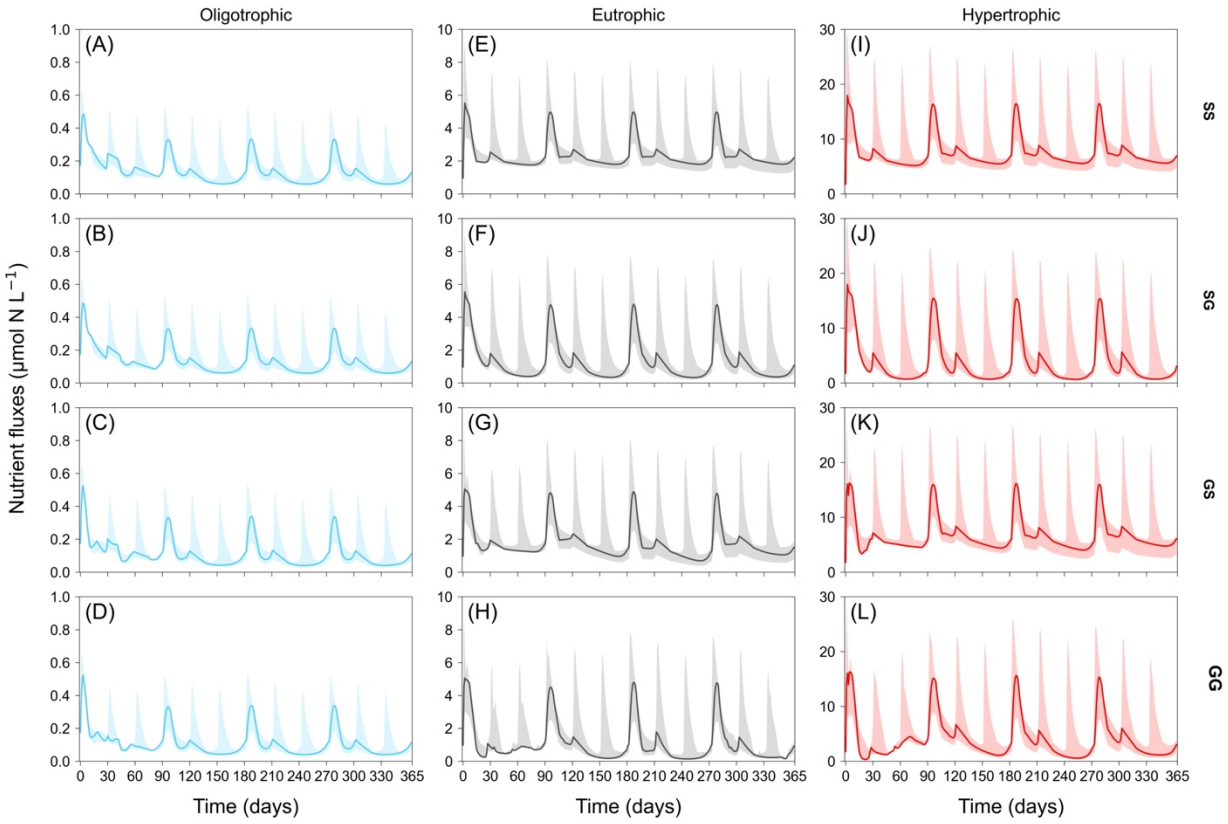

Figure S8. Nutrient fluxes over time, before uptake by phytoplankton, under varying mixing frequencies (shaded areas), for different nutrient regimes (by column) and grazing scenarios (by row). The continuous lines and the shaded areas represent, respectively, the median (50th percentile) and the interquartile range (i.e. the 25th and 75th percentiles) of the results obtained with the three mixing frequencies (constant, medium, and high). The plot shows the non-constant dynamics of nutrient before uptake and grazing take place (explaining minor differences between grazing scenarios), including only replenishment from detritus and differential effects from physical processes.

References

Banas, N.S., 2011. Adding complex trophic interactions to a size-spectral plankton model: Emergent diversity patterns and limits on predictability. Ecological Modelling 222, 2663–2675. https://doi.org/10.1016/j.ecolmodel.2011.05.018

Fasham, M.J.R., Ducklow, H.W., McKelvie, S.M., 1990. A nitrogen-based model of plankton dynamics in the oceanic mixed layer. j mar res 48, 591–639. https://doi.org/10.1357/002224090784984678

Hansen, B., Bjornsen, P.K., Hansen, P.J., 1994. The size ratio between planktonic predators and their prey. Limnology and Oceanography 39, 395–403. https://doi.org/10.4319/lo.1994.39.2.0395

Hansen, P.J., Bj, P.K., Hansen, B., 1997. Zooplankton grazing and growth: Scaling within the 2-2,000um body size range. Limnology and Oceanography 42, 687–704.

Layden, A., Merchant, C., MacCallum, S., 2015. Global climatology of surface water temperatures of large lakes by remote sensing: Global climatology of Lake Surface Water Temperatures. Int. J. Climatol. 35, 4464–4479. https://doi.org/10.1002/joc.4299

Oschlies, A., Schartau, M., 2005. Basin-scale performance of a locally optimized marine ecosystem model. J Mar Res 63, 335–358. https://doi.org/10.1357/0022240053693680

123